Geofísica Internacional (1999), Vol., 38, Num. 4, pp. 251-260

Numerical modeling of high-temperature deep wells in the Cerro Prieto geothermal field, Mexico

A. García[1], F. Ascencio[2], G. Espinosa[3], E. Santoyo[4], H. Gutiérrez[5] and V. Arellano[1]

[1] *Instituto de Investigaciones Eléctricas, Temixco, Morelos, México.*

[2] *Universidad Michoacana de San Nicolás Hidalgo, Morelia, Michoacán, México.*

[3] *Universidad Autónoma Metropolitana-Izatapalapa, México, D.F., México.*

[4] *Universidad Nacional Autónoma de México, Temixco, Morelos, México.*

[5] *Comisión Federal de Electricidad, Mexicali, B.C., México.*

Received: April 1, 1998; accepted: April 7, 1999.

RESUMEN

Se presenta un estudio de modelación numérica sobre las características de producción de tres pozos geotérmicos profundos del campo de Cerro Prieto, en cuya parte Este se perforaron seis pozos profundos (profundidad promedio de 4000 m) hace 15 años. El objetivo de este estudio es el cálculo de las características de producción de estos pozos para determinar si su incapacidad para mantener la producción se debió a (i) las pérdidas de calor del pozo, (ii) la influencia del diámetro de la tubería de producción, (iii) el efecto transitorio de la temperatura durante los primeros días de producción o (iv) la entrada de flujos secundarios de baja entalpía. Se desarrolló una nueva versión del simulador de flujo llamado GEOPOZO v2.0 que resuelve las ecuaciones de conservación de masa, momento y energía para flujo estable o transitorio de una y dos fases en pozos geotérmicos. Se encontró que los tres pozos estudiados deberían ser capaces de mantener la producción. Las pérdidas de calor tempranas fueron tan altas que los pozos requieren ser inducidos y solamente pueden mantener la producción después de varios días de inducción. La comparación con datos medidos en el pozo M-202 permitió la evaluación de los efectos de zonas secundarias de alimentación. Los ajustes logrados entre los perfiles medidos y calculados en el caso de una zona secundaria de alimentación permitió inferir que la entrada de agua más fría fue responsable de que el flujo en este pozo se detuviera.

PALABRAS CLAVE: pozos geotérmicos, simulación de flujo, perdidas de calor, zonas secundarias de alimentación, estimulación de pozos, inyección de gas.

ABSTRACT

A numerical modeling study of three non-producing deep geothermal wells from Cerro Prieto is presented. We compute the expected production characteristics of these wells in order to determine if their inability to sustain flow was due to (i) heat loss effects in the well, (ii) the influence of production casing diameters, (iii) the transient heat loss during the first few days of well discharge, or (iv) the effect of secondary low-enthalpy inflows. A new version of the wellbore flow simulator called GEOPOZO v2.0 was developed to solve the equations of conservation of mass, momentum and energy for steady or transient one- and two-phase flow in geothermal wells. It was found that all three wells should have sustained production. The early heat losses were so large that the wells need to be induced and they would only sustain flow after several days of induced discharge. For well M-202 the match between measured and computed temperature profiles for a secondary feedzone suggests that the inflow of colder waters was responsible for stopping the flow of this well.

KEY WORDS: geothermal wells, flow simulation, heat losses, secondary feedzones, well stimulation, gas injection.

INTRODUCTION

In a previous study (García, Santoyo and Hernández, 1992), the Comisión Federal de Electricidad (CFE-México) and the Instituto de Investigaciones Eléctricas (IIE-México) jointly developed a wellbore flow simulator called **GEOPOZO**. The simulator was initially applied to the study of well M-201 (3820 m total depth) at Cerro Prieto geothermal field in Baja California, Mexico to evaluate the effects of (i) heat transfer in the well-formation system; (ii) different casing diameters; (iii) transient heat loss during the first few days of discharge, and (iv) a low-enthalpy, secondary feedzone. However, the study was not based on real flow data since well M-201 had not sustained production.

Menzies *et al*., (1995) modeled the discharge requirements for deep wells in Cerro Prieto. They concluded that these wells can probably be induced to flow if a discharge rate of at least 300 liters/min can be sustained. If the sustainable rate from the well is closer to 60 liters/min, then it is unlikely that the well can be successfully stimulated in less than 20 days due to heat loss to the cold formation in the upper 1900 m of the well. Stimulation times of less than one day should be required, assuming a discharge rate of greater than 300 liters/min. In actual field operation, larger stimulation times of up to 11 days have been required. This difference was attributed to the assumption of continuous flow, which is not realistic. Nitrogen injection with a coiled tub-

ing was recommended for future discharge attempts.

In this paper we carry out simulation flow studies for wells M-201, M-202 and M-205 and we discuss the problems related to starting and sustaining production from these wells. Well M-201 was studied previously (García, Santoyo and Hernández, 1992). Well M-205 was the deepest well drilled in the field, and well M-202 produced geothermal fluids and had some field data available for this study.

The location of these wells is shown in Figure 1. The basic information for the M-200 series wells in Cerro Prieto is given by Menzies *et al*., (1995). Studies of other Cerro Prieto wells are described by Palacio-Pérez (1985), Chadka, Malin and Palacio-Pérez (1993) and Jasso and Peña (1990), among others.

THE GEOPOZO COMPUTER PROGRAM

A review of wellbore flow simulators is given by García *et al*., (1995). GEOPOZO is a general purpose wellbore simulator which can perform steady or pseudo-steady state calculations from top to bottom and vice versa under different thermodynamic conditions, i.e., single or two-phase including compressed liquid and superheated steam. It can also handle secondary feedzones and variable casing diameter. **GEOPOZO** is based on a homogeneous flow formulation neglecting slip between phases. It is appropriate for cases where pressure changes in the axial direction are smooth and where flow patterns are not well established.

GEOPOZO solves the conservation of mass, momentum and energy equations for steady one- and two-phase flows in geothermal wells (Wallis, 1969):

$$\left(\frac{dw}{dz}\right)=0 \tag{1}$$

$$\left(\frac{dp}{dz}\right)-\left[\left(\frac{dp}{dz}\right)_f+\left(\frac{dp}{dz}\right)_{ac}+\left(\frac{dp}{dz}\right)_g\right]=0 \tag{2}$$

$$w\left(\frac{de_t}{dz}\right)-Q=0 \tag{3}$$

where e_t is the specific total energy (enthalpy, kinetic and

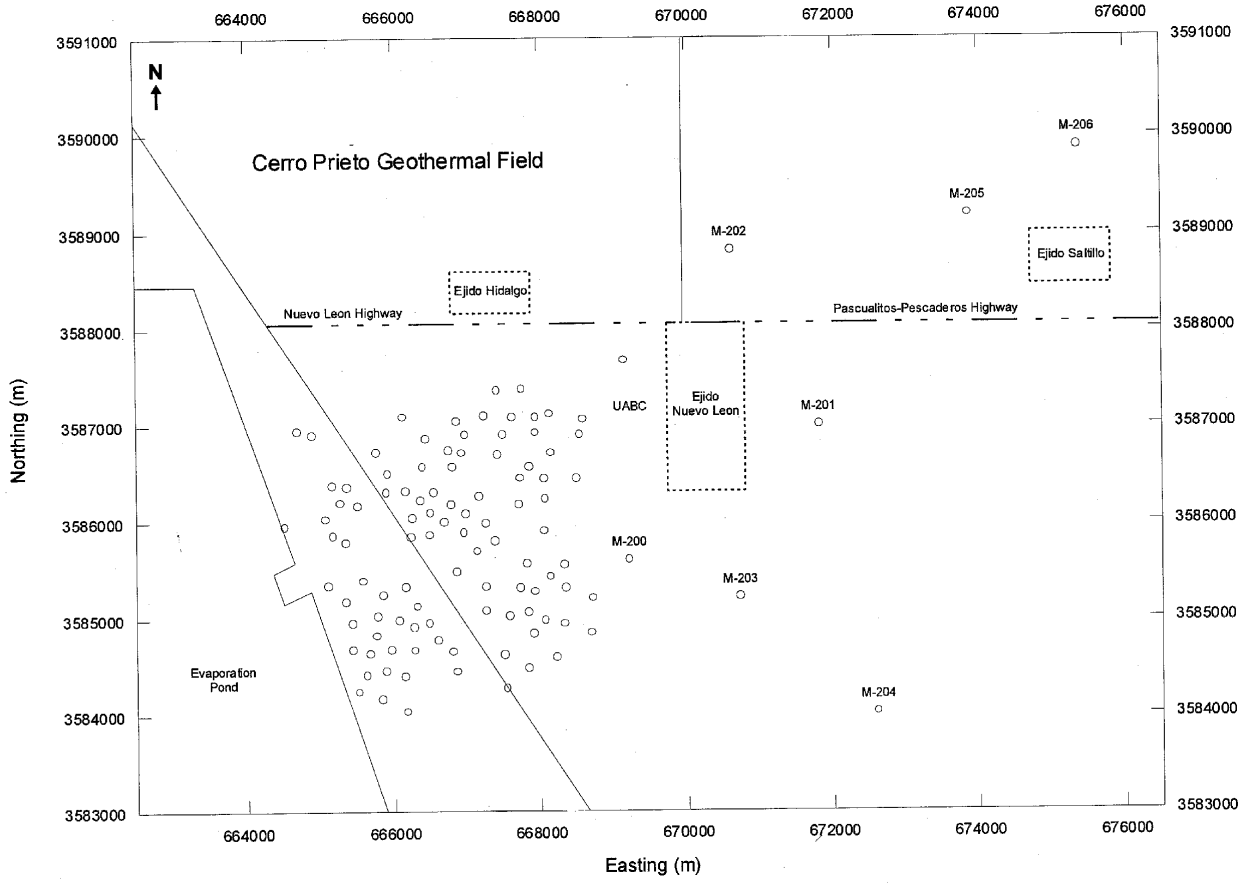

Fig. 1. Location of wells in the Cerro Prieto geothermal field. Coordinates are expressed in Universal Transverse Mercatur (UTM) units.

potential energy) and Q is the heat exchange between the well and the surrounding formation, w is mass flowrate, z is the vertical coordinate and p is pressure. The first term in the square brackets (Equation 2) represents pressure loss due to friction, the second denotes the pressure loss due to acceleration, and the third is the gravitational pressure loss. Detailed expressions for these terms can be found elsewhere (Wallis, 1969; García and Santoyo, 1991). Equations (1)-(3) are solved subject to the following boundary conditions:

$$w = \text{constant} \tag{4}$$

$$p = p_{wf} \qquad \text{at } z = z_{\max} \tag{5}$$

$$e_t = h_{res} + gz \qquad \text{at } z = z_{\max} \tag{6}$$

where p_{wf} is the bottomhole flowing pressure, h_{res} is the specific enthalpy of the reservoir and $z_{\max}$ is the maximum well depth. Single-phase friction factors are calculated (Sánchez, 1990) according to:

(i) laminar flow,

$$f_L = \frac{64}{\mathrm{Re}} \tag{7}$$

(ii) transition flow,

$$f_L = 10^{\left[260.67 - 228.62\,Re + 66.307\,Re^2 - 6.3944\,Re^3\right]} \tag{8}$$

(iii) turbulent flow,

$$\frac{1}{\sqrt{f_L}} = 2\log\left(\frac{1}{(\varepsilon/D)}\right) + 2\log\left(\frac{9.34}{(\varepsilon/D)\cdot Re\cdot\sqrt{f_L}}\right) + 1.14 \tag{9}$$

(iv) and highly turbulent flow,

$$f_L = 10^{\left[A + B\,EX + C\,EX^2 + D\,EX^3\right]}, \tag{10}$$

where A = -1.953, B=0.0518, C=3.64x10^{-3}, D=9.309x10^{-5}, and EX = $(\varepsilon/D)\cdot 10^{-4}$. Two-phase friction factors are considered constant and equal to $f = 0.025$ (Wallis, 1969). If a secondary feedzone occurs in the well, the total mass flowrate w_{tot} is given by

$$w_{tot} = w + w_{sec}\,, \tag{11}$$

where w is the main feed flowrate and w_{sec} is the secondary feedzone flowrate. If the reservoir pressure at the secondary inflow zone is unavailable, the pressure at the mixing point is assumed to occur at the inflow point in the well (Bjornsson, 1987):

$$p_j = p_{sec} \tag{12}$$

where p_j is the pressure at the depth of the secondary feedzone. Heat losses to the formation are calculated from the standard heat transfer equation

$$Q = U\,A\,\Delta T\,, \tag{13}$$

where U is the overall heat transfer coefficient, A is the area for heat transfer from the well to the surrounding rock and ΔT is the temperature difference between the fluid and the surrounding rock. The definition of U is given by Willhite (1967):

$$U = \frac{1}{\frac{1}{h} + \sum R_{th,c}}, \tag{14}$$

where h is the film heat transfer coefficient and $\Sigma R_{th,c}$ represents the sum of the conductive thermal resistances to heat flow due to the various casings and cemented zones.

The film heat transfer coefficient of Equation (14) is obtained from Gnielinski (1976):

$$Nu = \frac{(f/8)(Re - 1000)Pr}{1 + 12.7\sqrt{(f/8)}\,(Pr^{2/3} - 1)} \tag{15}$$

where $f = [1.82 \log (\mathrm{Re}) - 1.64]^{-2.}$

The temperature distribution in the surrounding formation assuming radial and transient heat conduction is

$$\frac{\partial T_r}{\partial t} = \frac{\alpha_r}{r}\frac{\partial}{\partial r}\left(r\frac{\partial T_r}{\partial r}\right), \tag{16}$$

where T_r is the temperature of the surrounding rock, α_r is the rock thermal diffusivity, r is the radial coordinate and t is time. Vertical heat conduction is neglected since radial temperature gradients are greater than vertical gradients (e.g., Figure 7 in Menzies *et al*., 1995). The latter would be more important if drilling fluid is lost to the formation (García *et al*., 1998). Boundary and initial conditions are:

$$T_r(t, r = r_w) = T_i \tag{17}$$

$$T_r(t, r = \infty) = T_g \tag{18}$$

$$T_r(r, t = 0) = T_g\,, \tag{19}$$

where T_g is the stable formation temperature as a function of depth, $T_g = f(z)$, T_i is the temperature of the fluid-rock interface which is obtained from Equation (13), and r_w is the well inner radius.

The above equations are solved using the following

complementary relations. Friction factors for one-phase flow are calculated from the Moody-Colebrook-White correlation (e.g., Sánchez, 1990) as described above, while film heat transfer coefficients are calculated from the Gnielinski (1976) correlation which is valid for $Re \geq 2300$. Rock thermal properties are based on measured values. Thermodynamic properties of pure water are taken from standard correlations (IFC, 1967; Meyer *et al*., 1968; Mercer and Faust, 1976; Leaver, 1984). The new version of the computer program covers the liquid region up to 45 MPa, the full two-phase region and the superheated steam region up to about 16.5 MPa and an enthalpy of 2565 kJ/kg. Minimum and maximum enthalpies are 109 kJ/kg and 3174 kJ/kg, respectively. **GEOPOZO** was validated against experimental data (García *et al*., 1995; Aragón *et al*., 1998) and against analytical solutions as discussed later. Further details can be found in García *et al*. (1993).

RESULTS

The Cerro Prieto wells M-201, M-202 and M-205 are three of six deep wells drilled in the eastern part of the geothermal field. They reached 4000 m depth and well M-205 reached nearly 4400 m. Figure 2 shows the completion and depths of the three wells that were studied.

WELL M-201

This well was completed with 9-5/8" casing from the surface to 2350 m, 7" casing from there until 3600 m and 4-1/2" liner down to 3820 m depth (Figure 2). M-201 did not flow and the results presented here were obtained using completion and reservoir data to simulate pseudo-transient flowing conditions. Reservoir data for this well were assumed as follows:

Pressure (p):	321 bar (depth = 3820 m)
Temperature (T):	350°C (depth = 3820 m)
Porosity:	0.15
Transmissivity (kH):	8 Darcy-m
Reservoir thickness:	300 m
Rock thermal conductivity:	1.7 W/m-K
Rock density:	2500 kg/m^3

The solid line in Figure 3 shows the static temperature profile. For the upper 1500 m, there is a small gradient of about 2°C/100 m, reaching some 40°C at 1500 m. In the next 2000 m, there is a substantial increase in gradient (14°C/100 m) corresponding to a conductive profile in the cap rock above the reservoir. Finally, the third change in geothermal gradient, below 3500 m depth, indicates the presence of the reservoir. This profile is typical of the eastern part of the Cerro Prieto geothermal field (Gutiérrez, 1993). Figure 3 shows several computed temperature profiles as function of time for a flowrate of 36 T/h. This rate was chosen as an example since heat transfer effects are more pronounced at this low rate. Frictional pressure loss effects are more pronounced at high flowrates. The wellhead temperature increases from 30°C to approximately 220°C in 10 days. Afterwards, the rate of temperature change decreases and at about 80-90 days it stabilizes.

Figure 4 shows the variation with time of the rate of

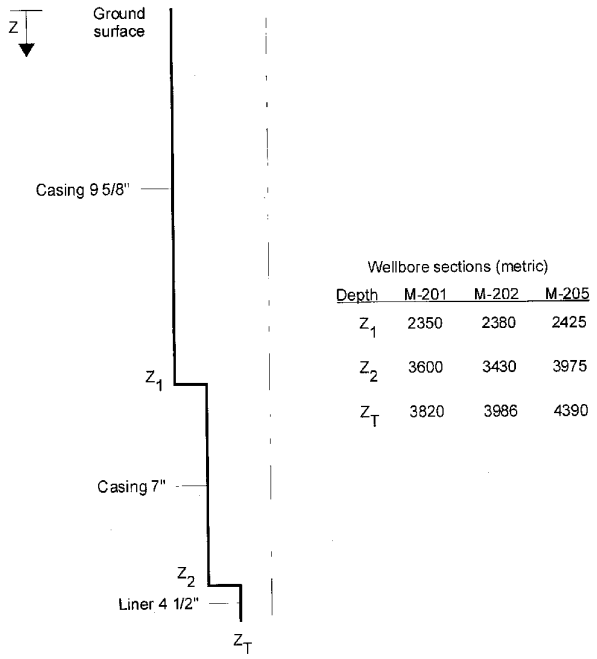

Fig. 2. Schematic diagram of the completion of the deep wells in the eastern part of the Cerro Prieto geothermal field.

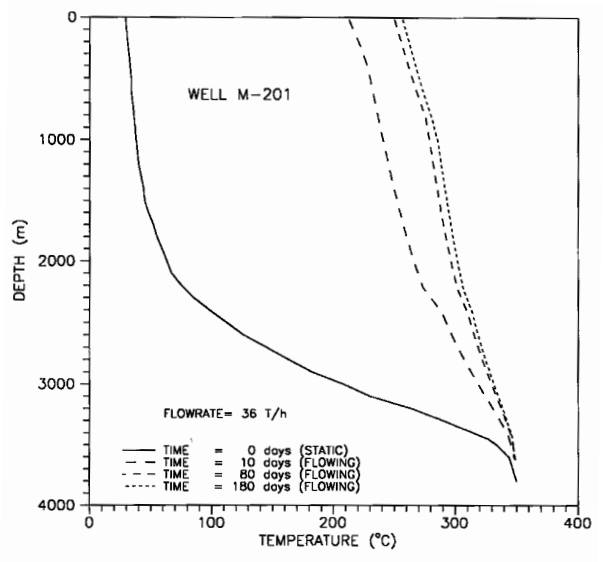

Fig. 3. Static and dynamic temperature profiles in well M-201.

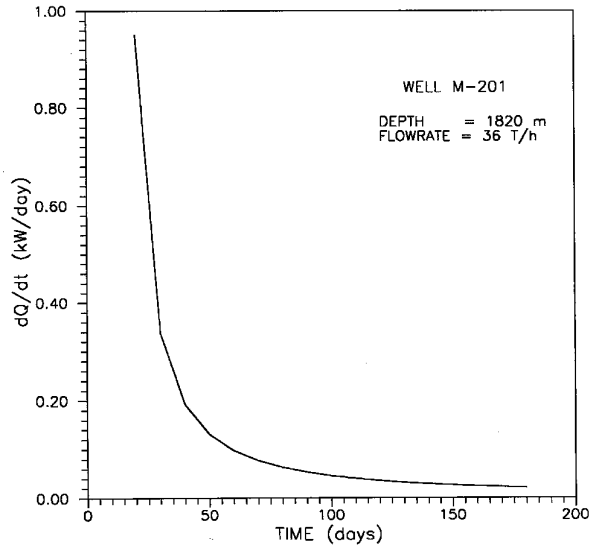

Fig. 4. Well M-201. Computed changes in heat loss with time.

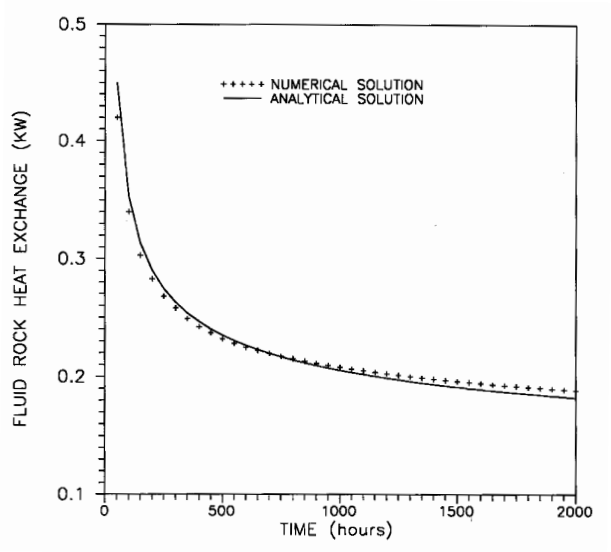

Fig. 5. Comparison of numerical and analytical heat losses as function of time.

change of heat losses for a flowrate of 36 T/h and a depth of 1820 m. Heat losses decrease rapidly during the first 40 days and then the rate of change is much slower. The rapid decrease in heat loss is due to the heating of the formation immediately surrounding the well. At large times, heat losses amount to a small but finite quantity (García and Santoyo, 1991). These findings are similar to those obtained by Menzies *et al*. (1995). Also, the formation remains unaltered far from the well, and the temperature profile in the well reaches steady-state conditions at large times.

Heat loss profiles were computed from the temperature field obtained from the solution of Equation (16), validated by comparison against the line source analytical solution (Ascencio, 1990):

$$Q = \frac{4\pi k_r (T_i - T_g)}{\ln\left(\dfrac{4\alpha_r t}{\sigma r_w^2}\right)} \quad , \qquad (20)$$

where T_i is the temperature of the fluid-rock interface, T_g is the geothermal temperature, k_r is the rock thermal conductivity, α_r is the rock thermal diffusivity, t is time, σ is Euler's constant (1.78) and r_w is the well inner radius.

Figure 5 shows a comparison of the numerical solution of Equation (16) with the analytical solution of Equation (20) for a case described by Ascencio (1990). Figure 6 shows the computed radial temperature profiles in the formation around well M-201 at 10, 60 and 120 days and at 820 m and 2820 m depth. The changes in rock temperature are small after 60 days. Actually, formation temperatures stabilize after about 90 days (García and Santoyo, 1991), and the penetration of the thermal disturbance reaches some 10 m into the formation.

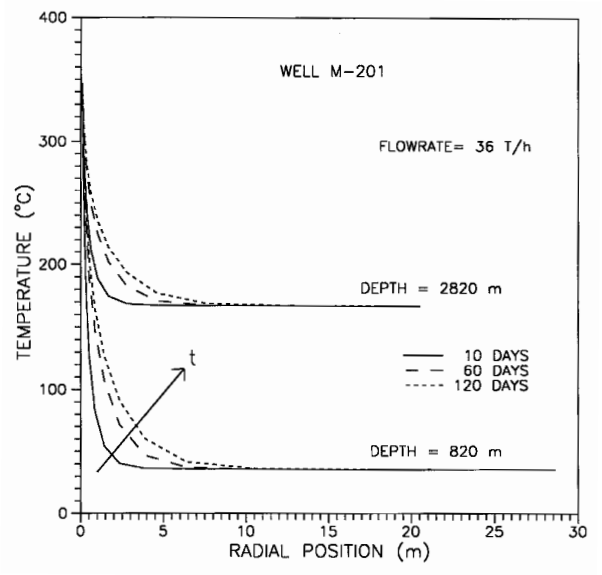

Fig. 6. Computed radial temperatures in the formation around well M-201.

The preceding figures suggest that heat transfer plays a major role during the first few days after the well starts flowing. The temperature gradient tends to decay rapidly, so that heat losses to the formation should not prevent the well from sustaining flow after a few days of induced discharge. Thermal stabilization is faster in the well and slower in the formation.

The effect of variable casing diameters (9-5/8", 7" and 4-1/2") versus constant diameter (7") on the M-201 pres-

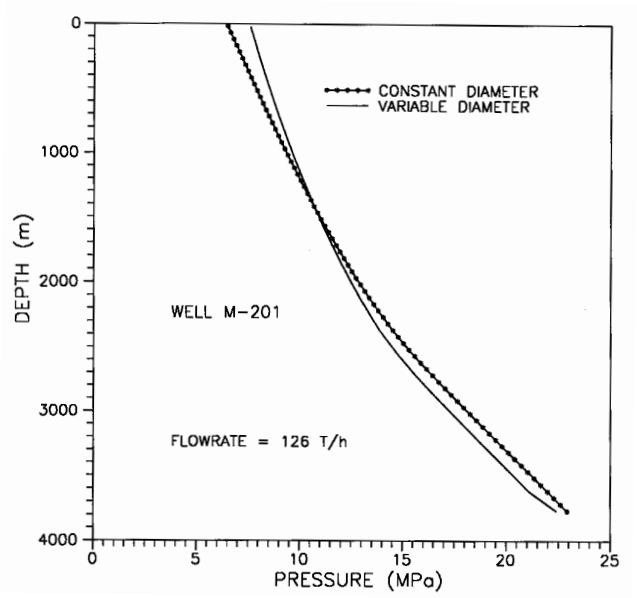

Fig. 7. Computed steady-state pressure profiles in well M-201 for variable (present) and constant (15.7 cm, 7") casing diameters.

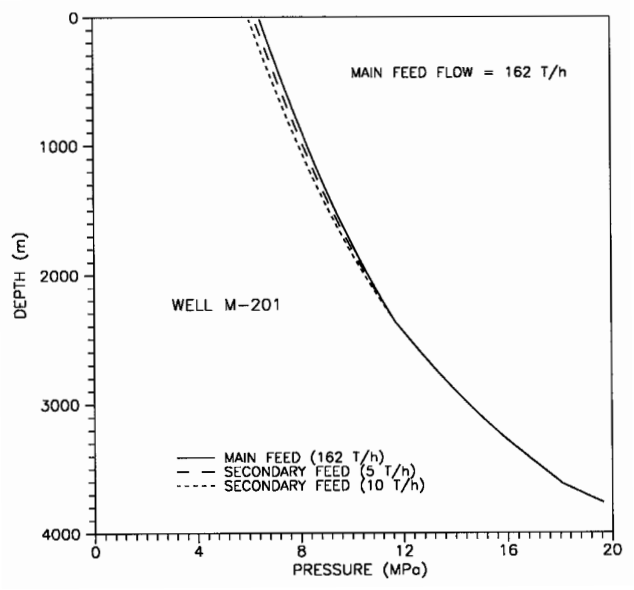

Fig. 8. Computed steady-state pressure profiles in well M-201 in the presence of flow from a secondary feedzone at 2350 m depth.

sure profile for a flowrate of 126 T/h is shown in Figure 7. In both cases, the wellhead pressure is significant. It is higher for the variable diameter case (76 bars versus 64 bars). Even though the flowrate (126 T/h) is an intermediate one, the wellhead pressure is high enough for the well to sustain production. These results are consistent with those of Garg and Combs (1997) who found that holes of diameters as small as 3" (79 mm) can sustain production although the produced rates are smaller than for larger diameter holes.

The effect of a secondary feedzone of temperature of 250°C on the steady-state pressure profile of well M-201 is shown in Figure 8. The assumed secondary feedzone flowrates are 5 and 10 T/h and reservoir flow equals 162 T/h. The zone is located at the point where the 9-5/8" and 7" casings overlap (2350 m depth). As the total flowrate increases from the point of mixing of the two streams, the pressure drop increases due to the combined effect of increased flowrate, i.e., increased friction, and lower average fluid temperature. However, wellhead pressures are not greatly affected by the inflow from the secondary feedzone. For the assumed conditions of the study, the well should also sustain flow.

We conclude that well M-201 may sustain flow in spite of heat losses. Additionally, Figure 9 shows the computed output curve for this well. It also shows that the well should sustain flow under normal operating conditions, with flowrates between about 20 and 180 T/h. Flow in this well could be induced by injecting air or nitrogen, as pointed out by Menzies *et al.* (1995).

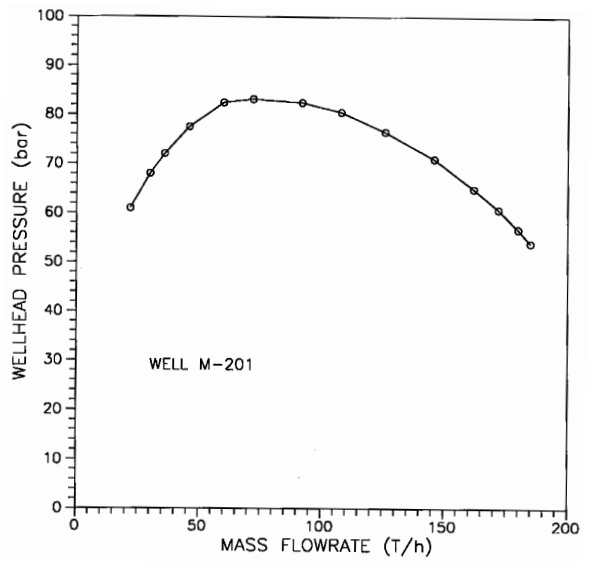

Fig. 9. Well M-201. Computed output curve.

WELL M-205

A similar study was performed for well M-205 which is the deepest geothermal well in Mexico. Its total depth is 4390 m. Its completion is shown in Figure 2 and the data used for its simulation is similar to that used for well M-201 (Ascencio, 1990). Figure 10 shows the computed output curve for M-205. It shows that under normal operating conditions the well should sustain flows between about 18 and 140 T/h,

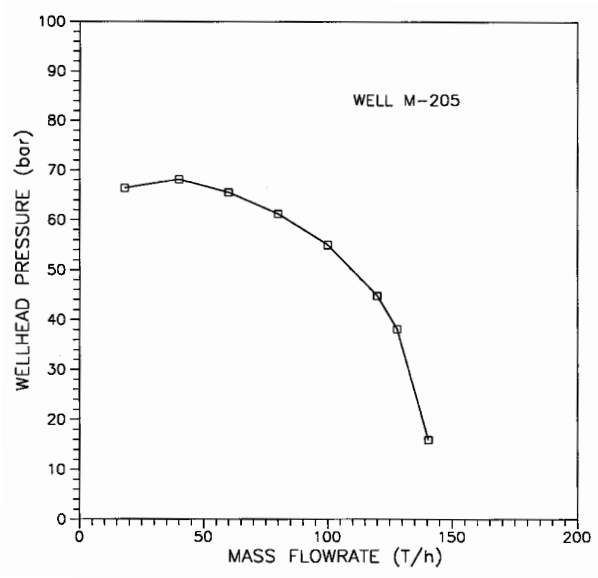

Fig. 10. Well M-205. Computed output curve.

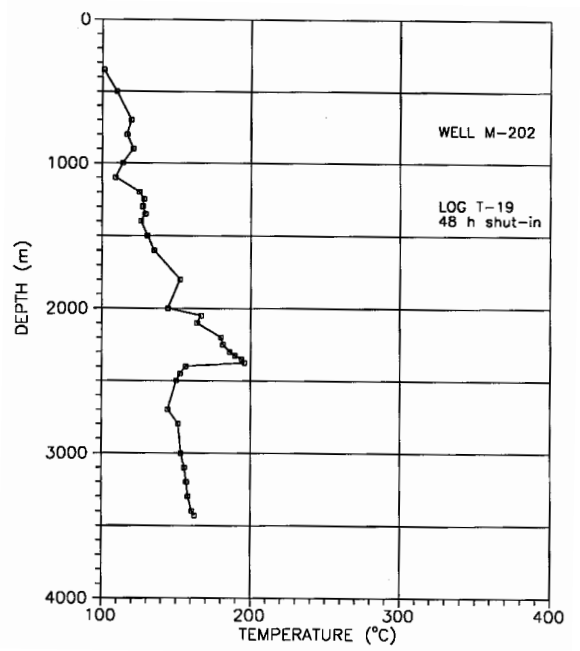

Fig. 11. Well M-202. Temperature profile (log T-19) measured 48 hours after the well stopped flowing.

with wellhead pressures as high as 68 bar. As with M-201. flow in this well could be induced by gas injection.

WELL M-202

Well M-202 was completed as shown in Figure 2. Its total depth is 3986 m and it exhibits the typical subsurface characteristics of the eastern part of the Cerro Prieto geothermal field (Figure 3). This well suddenly stopped flowing during discharge tests and this was attributed to a blockage due to sand invasion. A review of information including downhole temperature logs suggested that colder waters might have entered the well. The information also included drilling, discharge test data combined with flow simulation and comparison of measured and simulated data. Well M-202 was completed in June 1984 and was under observation for five months. The water level stabilized at 3020 m depth and temperature was 340°C at 3760 m. A caliper log showed resistance below that depth, possibly due to mud flocculation. No pressure logs were run. The discharge was then induced by air injection in November, and the well flowed at a wellhead pressure of 1 bar. By the end of December (1984), wellhead pressure was 39.7 bar. At the end of the heating period, the output curves were obtained. However, when flowing through a 0.114 m (4-1/2") orifice, the well became blocked with sand and flow stopped.

A caliper log was run through 0.157 m (7") to 2389 m; 0.146 m (5-3/4") to 3435 m, and 0.076 m (3") to 3735 m i.e. 250 m above total depth and inside the 0.114 m (4-1/2") liner. No anomalous situation was found. On January 4/5, 1985, temperature logs indicated cooling due to cold (150°C) water influx between the 9-5/8" casing and the 7" hanger, at about 2380 m depth. Repair was attempted but a 2695 m long, 0.114 m diameter drill pipe fish was not recovered.

Figure 11 shows a temperature log run 48 hours after the well stopped flowing. A 150°C secondary feedzone appears to be present at 2350 m approximately. Its flowrate may be determined with the aid of data from the previous test and mass and energy balances. Consider a reservoir flowrate w_1 at 340°C with an enthalpy of 1594 Kj/kg and a secondary feedzone with flowrate w_2 at 150°C with an enthalpy of 632 kJ/kg. The total mass flow rate at exit is

$$w_3 = w_1 + w_2 . \tag{21}$$

This equation is similar to Equation (11) which applies for the whole well. From the energy balance,

$$w_3 h_3 = w_1 h_1 + w_2 h_2 . \tag{22}$$

Equations (21) and (22) yield the expression from which the secondary feedzone flowrate was computed:

$$w_2 = \left(\frac{h_3 - h_1}{h_2 - h_1} \right) w_3 \quad \forall \ (h_3 > h_1). \tag{23}$$

Thus as the well is opened to higher flowrates, the secondary contribution increases. This, in turn, affects the production enthalpy.

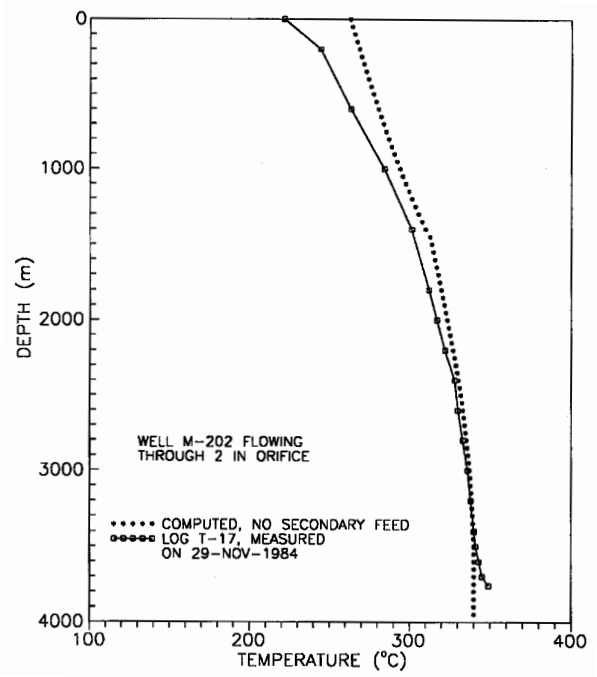

Fig. 12. Well M-202. Comparison of measured and computed temperature profiles without considering a secondary feedzone.

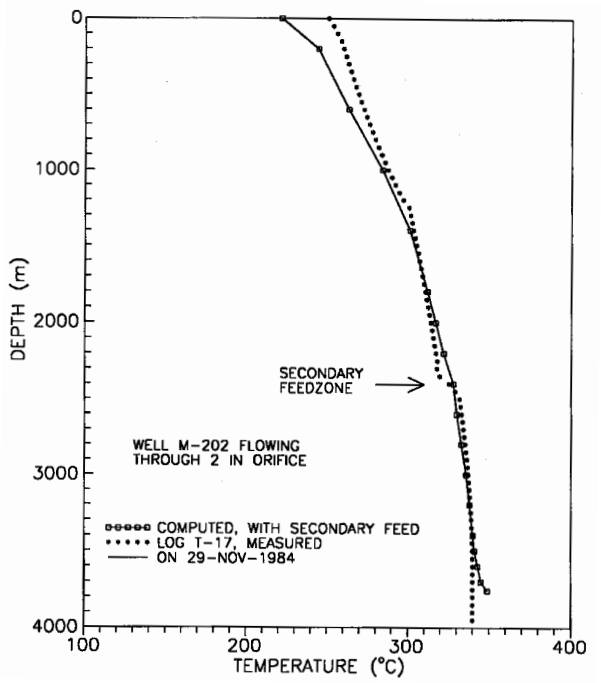

Fig. 13. Well M-202. Comparison of measured and computed temperature profiles considering a secondary feedzone at 3430 m depth.

Flow simulation

The GEOPOZO computer program was calibrated against measured data using log T-17 of Figure 12 which was run when well M-202 was flowing through a 0.05 m (2") purge. Since secondary feedzone flowrates were unknown, different flowrates were used to fit the measured profile. Figure 12 shows the calculated profile without considering a secondary feedzone. The measured profile is not reproduced satisfactorily. Now, 84% of total reservoir flow plus secondary feedzone flow were considered. The simulated and measured temperature profiles agree to within 8°C or less from the bottom of the well to about 1000 m (Figure 13). However, at shallow depths, agreement between calculated and measured temperatures was less good, as wellhead temperatures differed by as much as 30°C.

Reservoir and secondary feedzone flowrates were varied to study their effect on the resulting flowing pressure profiles. Figure 14 shows various simulated pressure profiles for well M-202 flowing through a 0.05 m (2") orifice for different secondary feedzone flowrates. As the cold water flowrate increases, wellhead pressure decreases, and for a secondary feedzone contribution of 6.2 kg/s (28.5% of the total flowrate), the wellhead pressure falls below atmospheric pressure and there is no wellhead fluid flow. Similar results were found from simulations for other orifice sizes (different total flowrates) employed during the discharge test of the well (Gutiérrez, 1993). Unfortunately, few experimental pressure data were collected during the discharge test.

In conclusion, the possible cause for the sudden death of well M-202 may have been the inflow of cold fluid and sand invasion, as originally reported. This finding agrees with Menzies *et al.*, (1995) who reported that well M-202 was killed by cool inflow from 7" liner lap. However, GEOPOZO does not allow the simulation of shut-in conditions which are more appropriate to study the static behavior of well M-202, (see Figure 11).

It is desirable to complement the simulation study described above with a numerical simulation of the static (shut-in) behavior of the well following a production period (Figure 11). The mismatch between simulated and measured values for the flowing case (Figure 13) indicates that the wellhead conditions derived from calculated results differ from the measured data. This is important when estimating output curves. Further work needs to be done to account for the temperature drops which were probably caused by shallower feedzones, as observed in Figure 11.

CONCLUSIONS

The 4000 m deep wells from the eastern part of the Cerro Prieto geothermal field should sustain flow in spite of

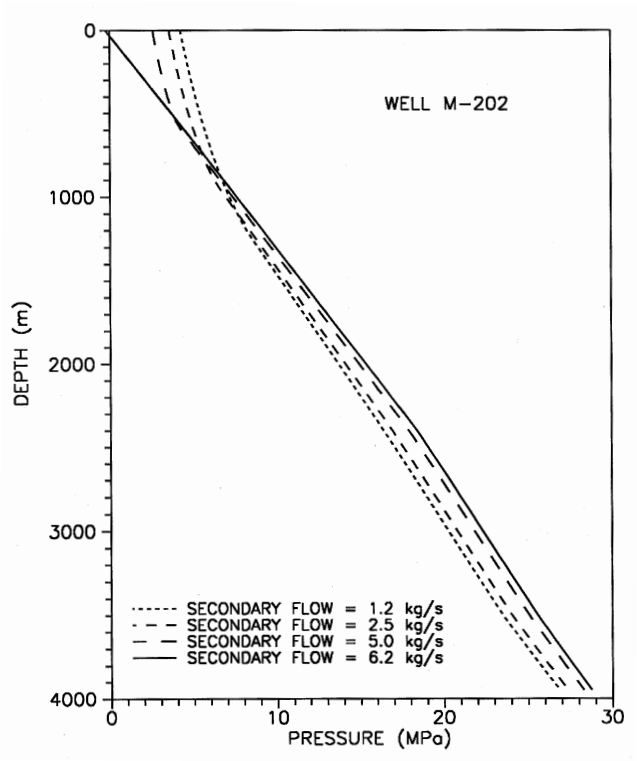

Fig. 14. Well M-202. Computed pressure profiles when flowing through a 5.1 cm (2") orifice with varying secondary feedzone flowrates.

large heat losses above 1500-2000 m depth, where the low rock temperature (< 100°C) gives rise to significant heat transfer from the well towards the formation. With time, the heat losses tend to decline to a small value. Stabilization of temperature is fast in the well but takes about 80-90 days for the rock. In particular, the study suggests that wells M-201 and M-205 of Cerro Prieto may sustain production flow under normal circumstances. Flowrates between 18-20 T/h and 140-180 T/h can be expected, with wellhead pressures as high as 70 to 84 bar. Flow could be induced by injecting air or nitrogen. A period of about 8-10 days of induction operations may be required for the wells to flow. This is consistent with the rapid temperature stabilization in the wells, the associated reduction in heat losses, and the results of similar studies on these same wells. It is likely that M-202 stopped flowing due to inflow of colder waters. When this inflow reached 25% or more of the total flow, the well stopped flowing.

ACKNOWLEDGEMENTS

The authors are grateful to Comisión Federal de Electricidad for assistance provided during this study; to Instituto de Investigaciones Eléctricas for permission to publish this work, and to the reviewers of the paper.

BIBLIOGRAPHY

ARAGON, A., A. GARCIA, A. BACA and E. GONZALEZ, 1999. Comparison of measured and simulated pressure and temperature (PT) profiles. *Geofís. Int., 38, 1,* 35-42.

ASCENCIO, F., 1990. Pronóstico de curvas características de producción. *Geotermia, Rev. Mex. Geoen., 6, 3,* 319-322.

BJORNSSON, G., 1987. A multi-feedzone geothermal wellbore simulator. MS Thesis, Univ. of California, Lawrence Berkeley Laboratory, USA, 102 pp.

CHADKA, P.K., M.R. MALIN and A. PALACIO-PEREZ, 1993. Modelling of two-phase flow inside geothermal wells. *Appl. Math. Modelling, 17,* 236-245.

GARCIA, A. and E. SANTOYO, 1991. Pronóstico de la producción del pozo M-205 del campo geotérmico de Cerro Prieto, B.C. Report of Project by Instituto de Investigaciones Eléctricas to Comisión Federal de Electricidad, Report IIE/11/3167/I 01/F, Cuernavaca, México.

GARCIA, A., E. SANTOYO and I. HERNANDEZ, 1992. GEOPOZO: Simulador de flujo bifásico en pozos geotérmicos. *In:* Memorias del XVIII Congreso de la Academia Nacional de Ingeniería, Aguascalientes, México, September, pp. 245-249.

GARCIA, A., I. HERNANDEZ and I. and V. VALENZUELA, 1993. Ampliación del rango de utilización del simulador GEOPOZO. Report of Project by Instituto de Investigaciones Eléctricas to Comisión Federal de Electricidad, Report IIE/11/5571/I 01/F, Cuernavaca, México.

GARCIA, A., H. GUTIERREZ, F. ASCENCIO, L. GONZALEZ, and J.M. MORALES, 1995. Wellbore flow simulation: Study cases of several Mexican wells. *In:* Proceedings, World Geothermal Congress, II, 1503-1511, Florence, Ita., May 18-31.

GARCIA, A., E. SANTOYO, G. ESPINOSA, I. HERNANDEZ and H. GUTIERREZ, 1998. Estimation of temperatures in geothermal wells during circulation and shut-in in the presence of lost circulation. *Transport in Porous Media, 33,* 103-127.

GARG, S. and COMBS, J., 1997. Use of slim holes with liquid feedzones for geothermal reservoir assessment. *Geothermics, 26,* 153-178.

GNIELINSKI, V., 1976. New equations for heat and mass transfer in turbulent pipe and channel flow. *Int. Chem. Engng*., *16*, 359-368.

GUTIERREZ, H., 1993. Estudio del pozo M-202 del campo geotérmico de Cerro Prieto. Report by Comisión Federal de Electricidad, Gerencia de Proyectos Geotermoeléctricos, Report OIY-CP-07/93, Morelia, Mich., México.

JASSO, C.A. and J.M. PEÑA, 1990. Evaluation of two-phase flow in geothermal well pipes utilizing the Orkiszewski model. *Geothermal Resources Council Transactions, 14, 1*, 415-421.

INTERNATIONAL FORMULATION COMMITTEE, IFC, 1967. The 1967 IFC formulation for industrial use: A formulation of the thermodynamic properties of ordinary water substance. Issued by the International Formulation Committee of the Sixth International Conference on the Properties of Steam, 32 pp.

LEAVER, J., 1984. Steam tables correlations (0-16 MPa). Unpublished report, Report by Ministry of Works and Development, New Zealand.

PALACIO-PEREZ, A., 1985. A computer code for determining the flow characteristics in a geothermal well. *In:* Proceedings of the Fourth International Conference on Numerical Methods in Thermal Problems, Swansea, U.K., July., 215-220.

MENZIES, A.J., E.E. GRANADOS, H. GUTIERREZ, and L. ORTEGA, L., 1995. Modeling discharge requirements for deep geothermal wells at the Cerro Prieto geothermal field, México. *In:* Proceedings of the 20th. Workshop on Geothermal Reservoir Engineering, Stanford, CA., 63-69.

MERCER, J.W. and C.R. FAUST, 1976. Simulation of water-and vapor-dominated hydrothermal reservoirs. *Soc. Petr. Engrs. of AIME,* Paper SPE 5520.

MEYER, C. A., R. B. MCCLINTOCK, G. J. SILVESTRI, and R.C. SPENCER, 1968. ASME Steam Tables. American Society of Mechanical Engineers, 2nd. ed., New York, 328 pp.

SANCHEZ, P., 1990. El simulador de pozos SIMU89. *Geotermia, Rev. Mex. Geoen*., *6*, 141-154.

WALLIS, G.B., 1969. One dimensional two-phase flow. McGraw-Hill Book Co., New York.

WILLHITE, G.P., 1967. Over-all heat transfer coefficients in steam and hot water injection wells. *J. Pet. Tech.*, 607-615.

A. García[1], F. Ascencio[2], G. Espinosa[3], E. Santoyo[4], H. Gutiérrez[5] and V. Arellano[1]

[1] *Instituto de Investigaciones Eléctricas, Unidad de Geotermia, Ave. Reforma 113, Col. Palmira, 62490 Temixco, Mor., México.*

[2] *Universidad Michoacana de San Nicolás Hidalgo, Escuela de Ingeniería Mecánica, Edif. W, Ciudad Universitaria, Morelia, Mich., México.*

[3] *Universidad Autónoma Metropolitana-Iztapalapa, Depto. IPH, Av. Michoacán y La Purísima, Col. Vicentina, 09430 México, D.F., México.*

[4] *Universidad Nacional Autónoma de México, Centro de Investigación de Energía, Priv. Xochicalco s/n, 62580 Temixco, Mor., México.*

[5] *Comisión Federal de Electricidad, Residencia General de Cerro Prieto; Ap. Postal 3-636; 21100 Mexicali, B.C., México.*